J Polym Environ (2012) 20:1–9
DOI 10.1007/s10924-011-0359-4

ORIGINAL PAPER

Poly(Lactic Acid) Blended with Cellulolytic Enzyme Lignin: Mechanical and Thermal Properties and Morphology Evaluation

Wenzhu Ouyang · Yong Huang · Hongjun Luo · Dongshan Wang

Published online: 16 September 2011

Abstract "Green"/bio-based blends of poly(lactic acid) (PLA) and cellulolytic enzyme lignin (CEL) were prepared by twin-screw extrusion blending. The mechanical and thermal properties and the morphology of the blends were investigated. It was found that the Young's modulus of the PLA/CEL blends is significantly higher than that of the neat PLA and the Shore hardness is also somewhat improved. However, the tensile strength, the elongation at break, and the impact strength are slightly decreased. Thermogravimetric analysis (TGA) shows that the thermal stability of the PLA is not significantly affected by the incorporation of the CEL, even with 40 wt% CEL. The results of FT-IR and SEM reveal that the CEL and the PLA are miscible and there are efficient interactions at the interfaces between them. These findings show that the CEL is a kind of feasible filler for the PLA-based blends.

Keywords Poly(lactic acid) · Celulolytic enzyme lignin · Extrusion · Blends · Biopolymer

W. Ouyang · Y. Huang · H. Luo · D. Wang
Laboratory of Cellulose and Lignocellulosics Chemistry, Guangzhou Institute of Chemistry, Chinese Academy of Sciences, Guangzhou 510650, China

W. Ouyang · H. Luo
Graduate University of Chinese Academy of Sciences, Beijing 100039, China

Y. Huang (✉)
National Engineering Research Center for Engineering Plastics, Technical Institute of Physics & Chemistry, Chinese Academy of Sciences, Beijing 100190, China
e-mail: yhuang@mail.ipc.ac.cn

Introduction

"Energy crisis" and "white pollution" urge us to reduce petroleum-based products, develop biomass resources, and recycle waste. Using biomass-based biodegradable plastics to replace traditional petroleum-based plastics is considered as one of the ultimate solutions to solve the environmental problems caused by using plastics and meet the sustainable development. However, several criteria such as reasonable cost, excellent mechanical properties, and harmlessness to animals and plants after biodegradation are required for these biodegradable plastics to meet the applications [1–3]. At present, some poly(aliphatic esters) such as PLA, poly(ε-caprolactone) (PCL), poly(butylene succinate) (PBS), polyhydroxyalkanoates (PHAs), together with biomass-based plastics like starch-based and cellulose-based ones, are interested in both industry and academia [4–6].

Compared to traditional plastics, however, the applications of biodegradable plastics are not so popular due to the limitation in varieties, properties and the high price [7]. In order to extend their applications, it is very important to solve these problems by chemical or physical modification, such as copolymerization, compounding, and blending. Polymer blending is usually thought to be a cheaper and less time-consuming process compared to exploring new polymerization routes or developing new polymers [8]; therefore it is widely used as an effective method in modification of polymer materials [9]. Usually, properties of blends are governed by the components in the blends and the interfacial interactions between them [10].

PLA is a polycondensate of lactic acid, which is derived from renewable agricultural products such as potato and corn. There is no environmental pollution

caused by the process in compounding and consuming PLA. Owing to the lower price and better thermal processing properties, compared to other biodegradable polymers, PLA is thought to be one of the most promising environmentally friendly polymer materials in sustainable development [4, 11]. So far, numerous PLA-based blends have been investigated, for example, PLA/polyester [12–15], PLA/starch [16–21], PLA/fibre [16, 22–25], PLA/chitosan [26, 27], and some ternary blends [28–32]; but, in most of these blends, compatibilizer should be added to enhance the interaction between the components in the blends, and the costs of these PLA-based materials are relatively high and some properties are also significantly affected in some cases.

Biomass is the largest resource in nature, of which the main components are cellulose, lignin, and semicellulose. Cellulose has been deeply studied and its products have been widely used. In contrast, lignin, the second largest component of the biomass, is less studied due to its structural complexity and denaturations, resulting in limited utilization of lignin. More than 70 million tons of lignin is annually generated as residue from chemical pulp mills [33], but only less than 5% of the lignin is used as chemicals or materials. In fact, there are many functional groups on the lignin molecules; therefore, the lignin is a promising material as a chemical component or as an organic filler in polymer blending. Also, the lignin reduces the cost of the final products and brings biodegradable characteristic to the thermoplastic polymers. Recently, many investigations on the properties of lignin/polyolefine blends have been reported, but there are only a few investigations on blending lignin with biodegradable polyesters [3, 11, 34, 35]. Inour et al. [11] has reported that the thermal and mechanical properties of the PLLA/lignin sulfonate blends are decreased greatly when the content of lignin is more than 20 wt%. It is a great challenge to obtain lignin/plastics blends with improved mechanical properties.

Cellulolytic enzyme lignin (CEL) is a byproduct in the bio-alcohol industry. Producing one ton bio-alcohol usually gives one ton CEL, i.e., lignocellulosic ethanol industries generate massive amounts of lignin. Therefore, the disposal of CEL is also one of the key problems for the bio-alcohol industry. In this study, we will focus on lowering the cost of PLA-based blends by using CEL as cheap filler with no significantly sacrificing their thermal and mechanical properties. The blending of the CEL with PLA also improved the Yang's modulus and the Shore hardness of the product, and the value-added application of CEL is achieved as well. The effect of CEL content on the thermal and mechanical properties of the blends and the compatibility between them were investigated.

Experimental

Materials

PLA (white granule, injection grade, weight average molecular weight $M_w = 1.66 \times 10^5$, polydispersity index $M_w/M_n = 1.95$), was purchased from Shenzhen Esun New Materials Co., Ltd. and dried at 80 °C in a drum oven for 20 h prior to processing. CEL was kindly supplied by Professor Yong Qiang in Nanjing University of Forest. It is a byproduct of bioethanol fabrication and its major component was lignin, along with some undegraded cellulose. The CEL was grounded into powder, sieved with sieves between 55 and 300 mesh, and dried in a drum oven at 80 °C for 48 h before use. The particle size distribution of the CEL measured by a laser scattering particle size distribution analyzer (LA- 950, HORIBA, Japan) is shown in Fig. 1.

Preparation of PLA/CEL Blends

Dried CEL powders and PLA granules were weighted separately according to the proportion and placed in a plate for thoroughly manual mixing. The mixture was subsequently fed into a TE-35 twin-screw extruder with an L/D of 44 (Nanjing Keya Co., China). The temperatures of the seven zones and the head section of the extruder were set at 165, 170, 170, 175, 180, 180, 165, and 175 °C, respectively, and the feeding speed was fixed at 398 rpm. The strands of the extrudate were then chopped into pellets and collected. The pelletized blends were dried in a convection oven at 80 °C for 24 h prior to injection molding, which was carried out on a HTF86X1 injection molder (131 cm^3 capacity, Ningbo Haitian Plastics Machinery Group Co.). The temperatures of the four zones and the nozzle temperatures were set at 185, 180, 175, 170, and 185 °C, respectively. The sample was cooled for 50 s, during that process the hold, pack, and fill pressures were maintained at 60, 65, and 68 MPa, respectively. Finally, the coupons were aged 24 h at room temperature before mechanical test.

Mechanical Measurement

Tensile measurement was performed according to ASTM D 638 on a universal testing machine RGM-3030 (30kN, Shenzhen Reger Instrument Co., Ltd., China). The crosshead speed was 5 mm min^{-1} and the sizes of the specimens were $150 \times 10 \times 4$ mm^3. Young's modulus was obtained by fitting the slope from the stress–strain curve. Notched izod impact testing was conducted following ASTM D 256 on a pendulum impact testing machine B 51113.300 (Zwick/Roell, Germany) at room temperature. All the samples were the injection molded coupons of $80 \times 10 \times 4$ mm^3 with a notch of 2 mm in depth. All data

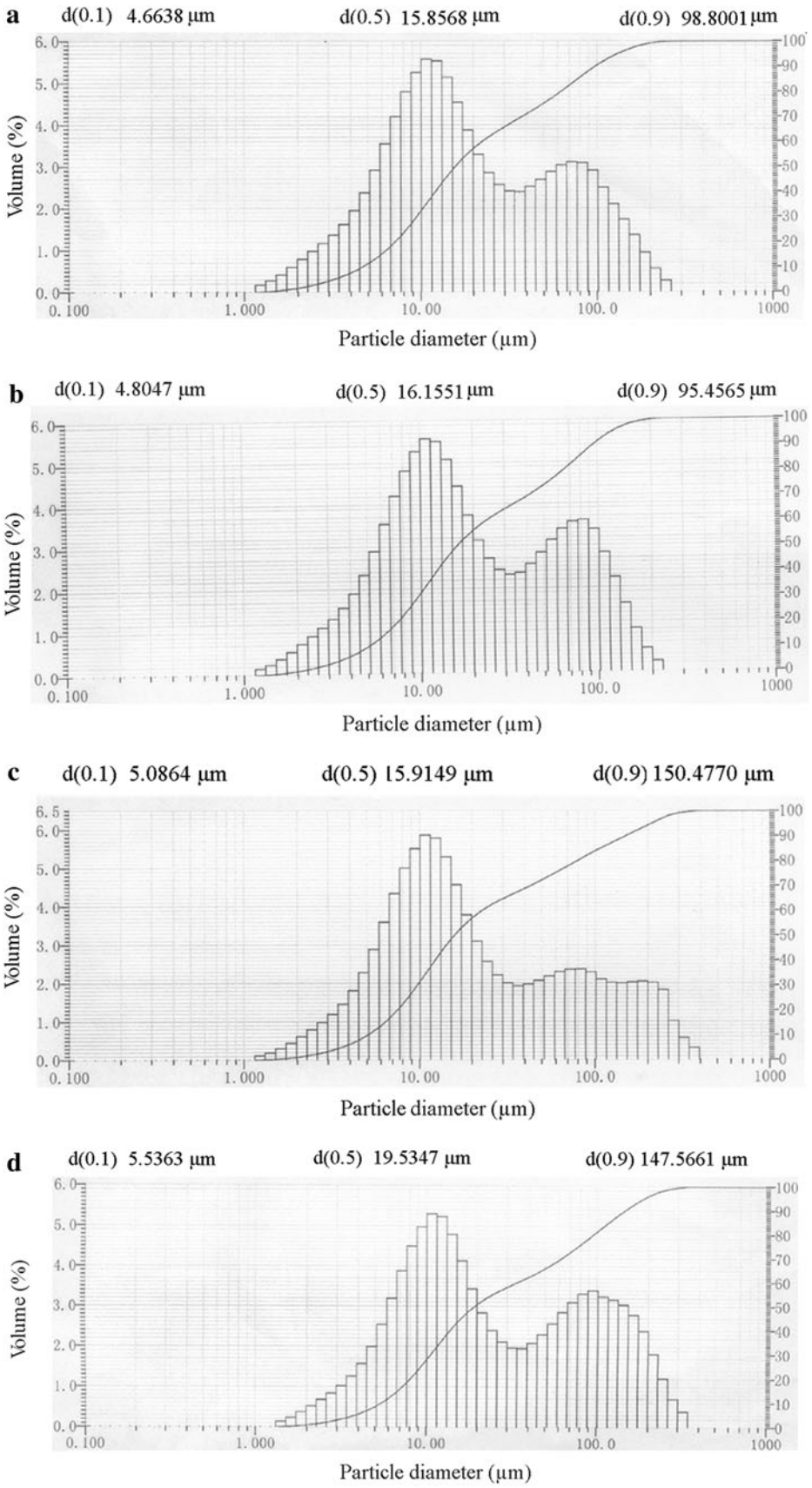

Fig. 1 Size distribution of CEL particles obtained with different sieves: **a** 300 mesh, **b** 200 mesh, **c** 100 mesh, and **d** 55 mesh

presented here were the average value of five measurements.

The hardness was determined according to ASTM D2240 with a Shore durometer. All the samples have size of 118 × 15 × 10 mm^3. The data were the average values of five measurements obtained from different positions on one specimen.

Thermogravimetry Analysis (TGA)

TGA was carried out with TGA2050 (TA Instruments, USA). The samples were scanned from 50 to 500 °C at a heating rate of 10 °C min^{-1} in nitrogen atmosphere.

Scanning Electron Microscopy (SEM)

The morphology of PLA/CEL blends was observed by an environmental scanning electron microscope (Quanta 400, FEI Co., USA) at room temperature. The freeze-fractured specimens were cryogenically frozen with liquid nitrogen.

Fourier-Transform Infrared (FT-IR)

IR measurements were carried out on a single-beam IR spectrometer (Nicolet-760, USA) at room temperature under nitrogen purging. All the samples were mixed with KBr and prepared into a thin disk under high pressure. Spectra were recorded from 400 to 4,000 cm^{-1} at a resolution of 4 cm^{-1} and with an accumulation of 32 scans.

Results and Discussion

Dispersal of each component in the blends and the interfacial interaction between them play an important role in properties for the blends. In order to know the dispersal of CEL sieved with different sieves in the PLA and the interaction between CEL and PLA, morphology of PLA/CEL (95/5, w/w) blends, in which the CEL is sieved with sieves between 55 and 300 mesh, is firstly investigated. Figure 2 shows the SEM micrographs of the freeze-fractured surfaces. It can be seen that all the CEL particles are uniformly dispersed in the PLA matrix and no obvious CEL aggregation can be found. Except for major lignin, CEL also contains some microcrystalline cellulose, but, it is difficult to find spherical particles lignin or microcrystalline cellulose fiber. However, in some other research reports [22, 37], cellulose fiber is noticeable. This suggests that the CEL can be well dispersed in PLA matrix after extrusion process and there is a good adhesion between the CEL and the PLA. However, the unconspicuous difference among the morphology of the blends with CEL sieved with different sieves between 55 and 300 mesh must be attributed to the pretty much particle size distribution of the CEL (see Fig. 1). Therefore, in this paper, the CEL sieved with 55 meshes was used directly to prepare PLA/CEL blends and the properties of these blends with different CEL contents were investigated.

PLA is a biodegradable polymer with high strength and high modulus, yet it is too expensive to be used extensively. The aim of this paper is to develop the value-added application of CEL in PLA-based materials and investigate the changes in thermal and mechanical properties of the PLA/CEL blends, in which CEL is low-cost. Figure 3 shows the stress–strain curves of the neat PLA and the PLA/CEL blends, from which we can obtain the tensile strength, the Young's modulus, and the elongation at break. Figure 4 shows that the tensile strength is decreased with increasing the CEL content in the blends, while the Young's modulus is kept increasing before the CEL fraction reaches 30 wt%. According to the data shown in Table 1, the tensile strength is decreased from 63.8 MPa for neat PLA to 40.1 MPa for the blend with 40 wt% CEL. The decrease of the tensile strength is less than 36%, which is much lower than 66% calculated from Inour's work [11]. On the other hand, the Young's modulus is increased with blending with CEL in our work, while it remains almost constant in Inour's report [11]. The lignin in CEL is a highly functionalized biomacromolecule, having primarily alkyl-aryl ether linkages, aliphatic, aromatic hydroxyl groups, relatively smaller molecular weight and lower polydispersity. The good retainment in tensile strength and the improvement in Young's modulus should be attributed to the highly functionalized structure of CEL. The hydroxyl groups of CEL can form hydrogen bonds with the carbonyl groups in PLA, and therefore enhancing the miscibility between the PLA and the CEL. The decrease of tensile strength for the blends may result from the lower tensile strength of CEL compared to that of the PLA. The increase of Young's modulus may be attributed to the rigid CEL component, which enhances the rigidity of the blends. But when the CEL is up to 40 wt%, the continuous phase of PLA might be seriously disrupted, leading to drop in the Young's modulus.

Figure 5 exhibits the variation of the elongation at break with the CEL content in the PLA/CEL blends. It can be seen that the elongation is decreased with increasing the CEL content. This result may also result from the rigidity of the CEL particles. Figure 6 shows the impact strength of neat PLA and the PLA/CEL blends with different contents of CEL. It can be seen that, due to the intrinsic brittleness of the PLA and the rigidity of the CEL, all the samples show low impact strength. However, the impact strength for each blend is only slightly lower than that of neat PLA, indicating that the impact strength of the blends is not obviously affected by the incorporation of the CEL. For

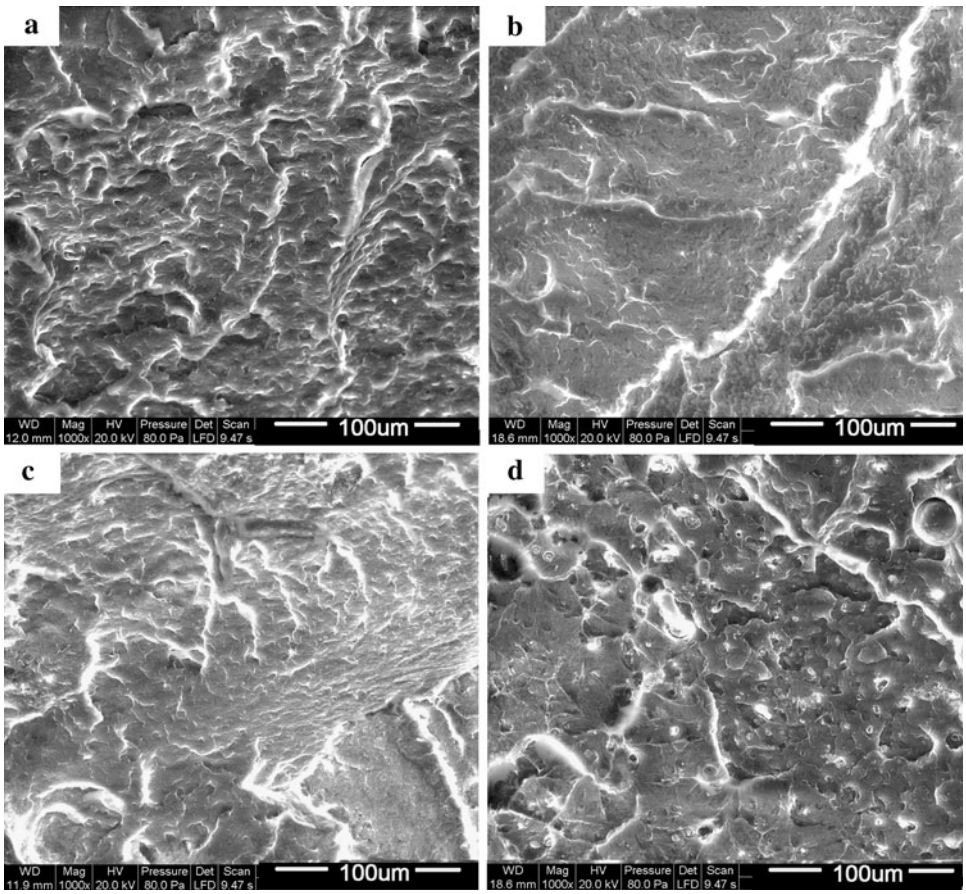

Fig. 2 SEM micrographs of freeze-fractured surfaces of PLA/CEL (95/5, w/w) blends with CEL particles obtained with different sieves: **a** 300 mesh, **b** 200 mesh, **c** 100 mesh, and **d** 55 mesh

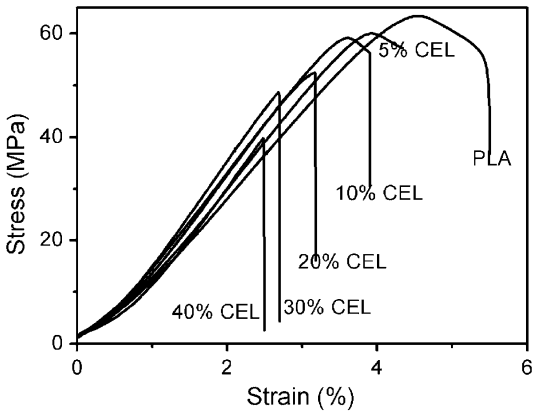

Fig. 3 Stress–strain *curves* of neat PLA and CEL/PLA blends

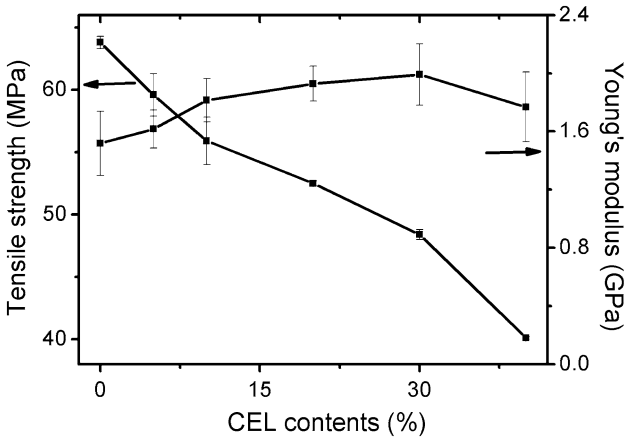

Fig. 4 Tensile strength and Young's modulus of PLA/CEL blends with different CEL contents

example, there is a drop of 0.3 kJ m^{-2} happened to the blend with 40 wt% CEL (Table 1), which is only decreased by 17.6% compared to a neat PLA sample. The retainment in impact strength also implies good miscibility and strong adhesion between the CEL filler and the PLA matrix.

In addition, PLA is also a plastic with high hardness. Figure 7 shows the Shore hardness of the neat PLA and its blends with CEL. It can be seen that, owing to the addition of rigid filler and the good miscibility between the CEL and the PLA, the Shore hardness is initially increased with increasing CEL content. But, when the CEL content reaches 40 wt%, the shore hardness is sharply decreased. This result is consistent with the variation of Young's modulus as the function of CEL in the blend. Maybe a similar explanation can be applied here. That is to say, the initial increase of hardness is also attributed to the rigidity of the CEL component, but with too much CEL added in

Table 1 Mechanical properties of PLA and its blends with CEL

Samples	Maximum strength (MPa)	Young's modulus (GPa)	Elongation at break (%)	Notched impact strength (kJ m^{-2})	Shore hardness (HD)
PLA	63.8 ± 0.5	1.52 ± 0.22	5.40 ± 0.65	1.7 ± 0.01	83.1 ± 0.2
PLA/5% CEL	59.6 ± 1.7	1.62 ± 0.13	4.60 ± 0.21	1.5 ± 0.11	84.0 ± 0.4
PLA/10%CEL	55.9 ± 1.9	1.82 ± 0.15	3.89 ± 0.13	1.5 ± 0.02	84.1 ± 0.3
PLA/20%CEL	52.5 ± 0.2	1.83 ± 0.12	3.16 ± 0.10	1.5 ± 0.01	86.0 ± 0.4
PLA/30%CEL	48.4 ± 0.4	1.99 ± 0.21	2.69 ± 0.09	1.4 ± 0.09	85.9 ± 0.6
PLA/40%CEL	40.1 ± 0.1	1.77 ± 0.24	2.42 ± 0.09	1.4 ± 0.02	83.0 ± 0.2

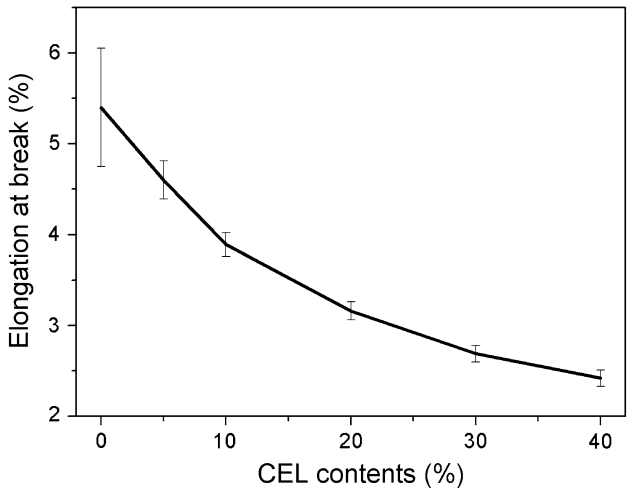

Fig. 5 Elongation at break of PLA/CEL blends with different CEL contents

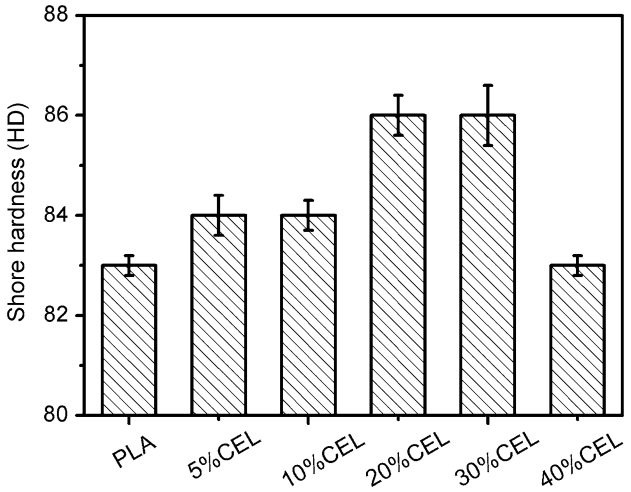

Fig. 7 Shore hardness of neat PLA and PLA/CEL blends

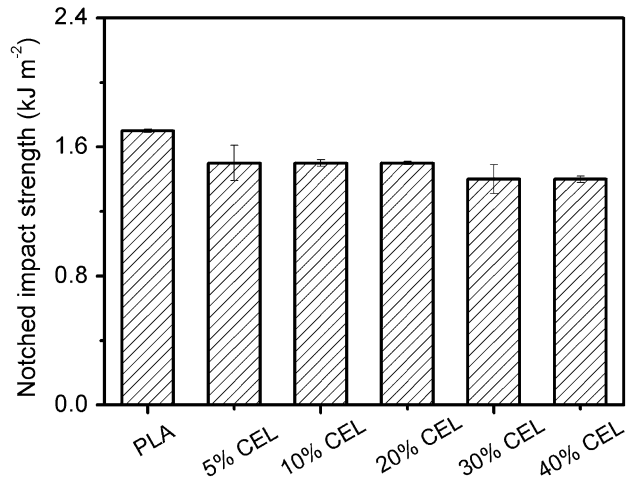

Fig. 6 Impact strength of PLA/CEL blends with different CEL contents

the system, the continuous phase of PLA is seriously disrupted, which leads to the drop in hardness for the blend with 40 wt% CEL.

Thermogravimetry (TG) is a useful method to monitor the process of thermal degradation of substances. The effect of CEL content on the thermal degradation of the PLA was shown in Fig. 8. Except for dehydration and carbon burning, there are two stages for CEL to decompose, corresponding to the two peaks on the DTG curve. The one at about 325 °C is attributed to the decomposition of lignin, and the other one at about 390 °C is attributed to the degradation of cellulose [36]. However, there is only one peak at about 360 °C on the DTG curve observed for the neat PLA to decompose completely. For the blends, there are also two peaks at about 360 and 425 °C on their corresponding DTG curves, indicating that not only the temperature of maximum thermal degradation rate (T_{max}) of the PLA is not affected by the CEL addition, but also T_{max} of the CEL components is improved. And from the TG curves, it can also be found that the point of the starting thermal decomposition for the PLA is not obviously affected by addition of CEL. For example, the starting point of the decomposition for the blend with 40 wt% CEL is only 3.4 °C lower than that of the neat PLA, and that is far lower than that in the previous work [11]. It is believed

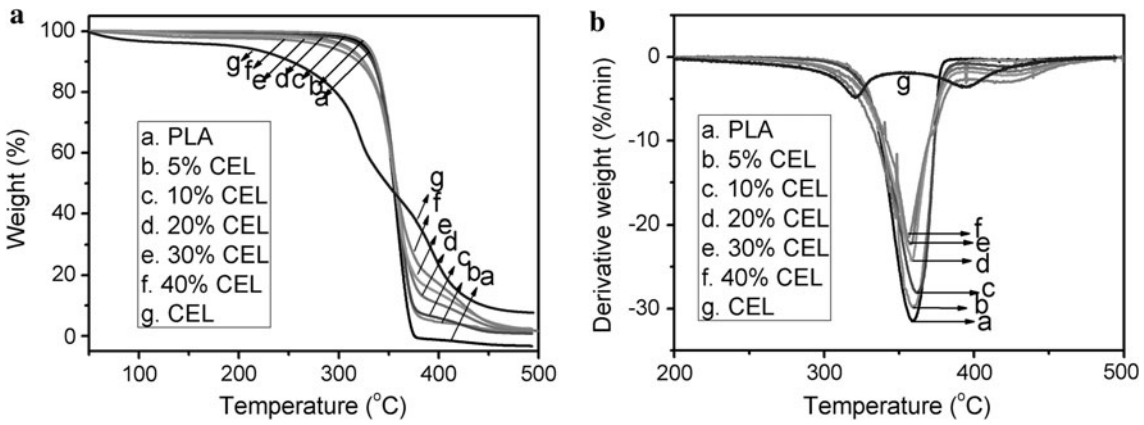

Fig. 8 TG and DTG *curves* of PLA, CEL, and PLA/CEL blends

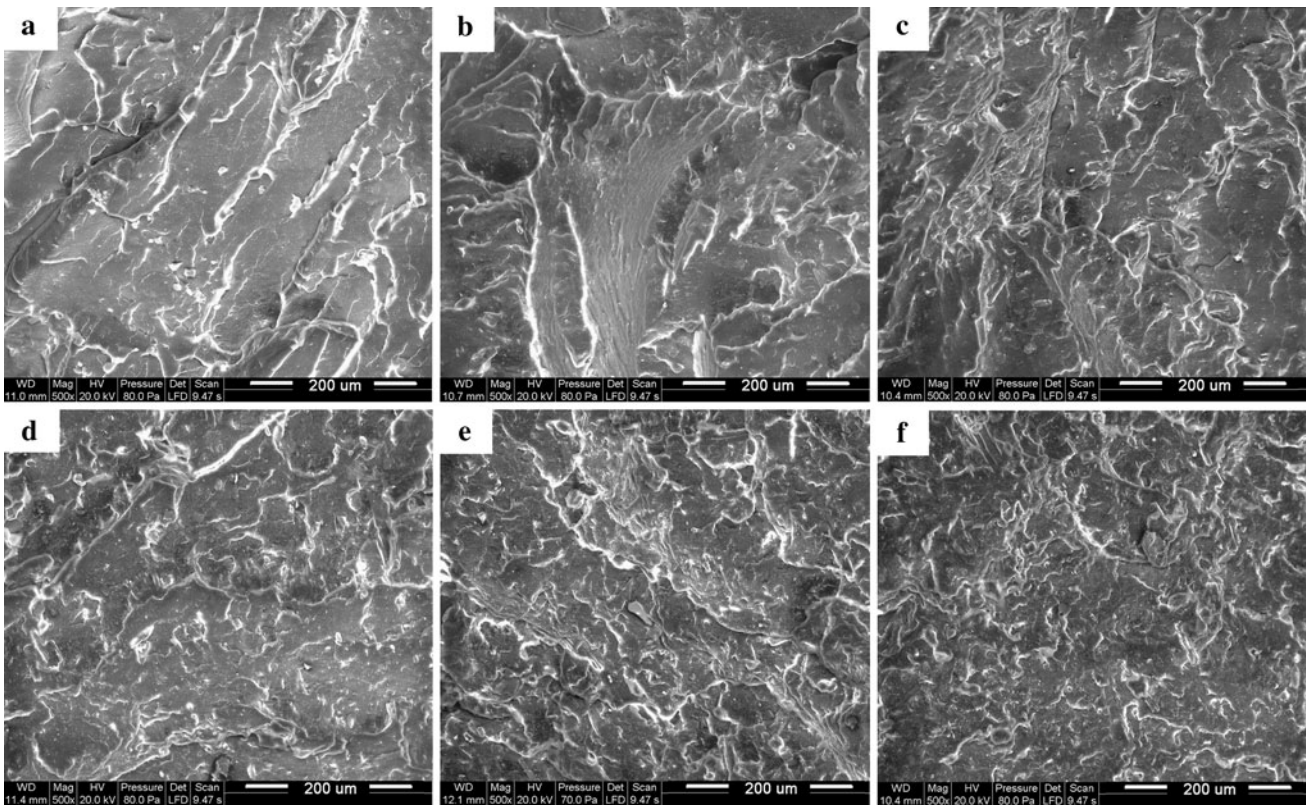

Fig. 9 SEM micrographs of freeze-fractured surfaces of PLA/CEL blends with various weight contents of CEL: **a** 0%, **b** 5%, **c** 10%, **d** 20%, **e** 30%, and **f** 40%

that the hydroxyl groups on the CEL enhance the compatibility of the PLA matrix and the CEL filler, resulting in good retention of thermal properties.

Figure 9 shows the morphology of freeze-fractured surfaces of neat PLA and the PLA/CEL blends with different CEL contents. It can be found that, with the CEL content increasing, the effective cross sectional area of the continuous PLA phase is reduced, but the whole morphology is homogeneous and there is no CEL particles observed from the freeze-fractured surface, even CEL content up to 40 wt%. It is confirmed that the compatibility between the CEL and the PLA is relatively perfect and there is a good adhesion or interaction between the PLA and the CEL. Perhaps, it is the strong hydrogen bonds

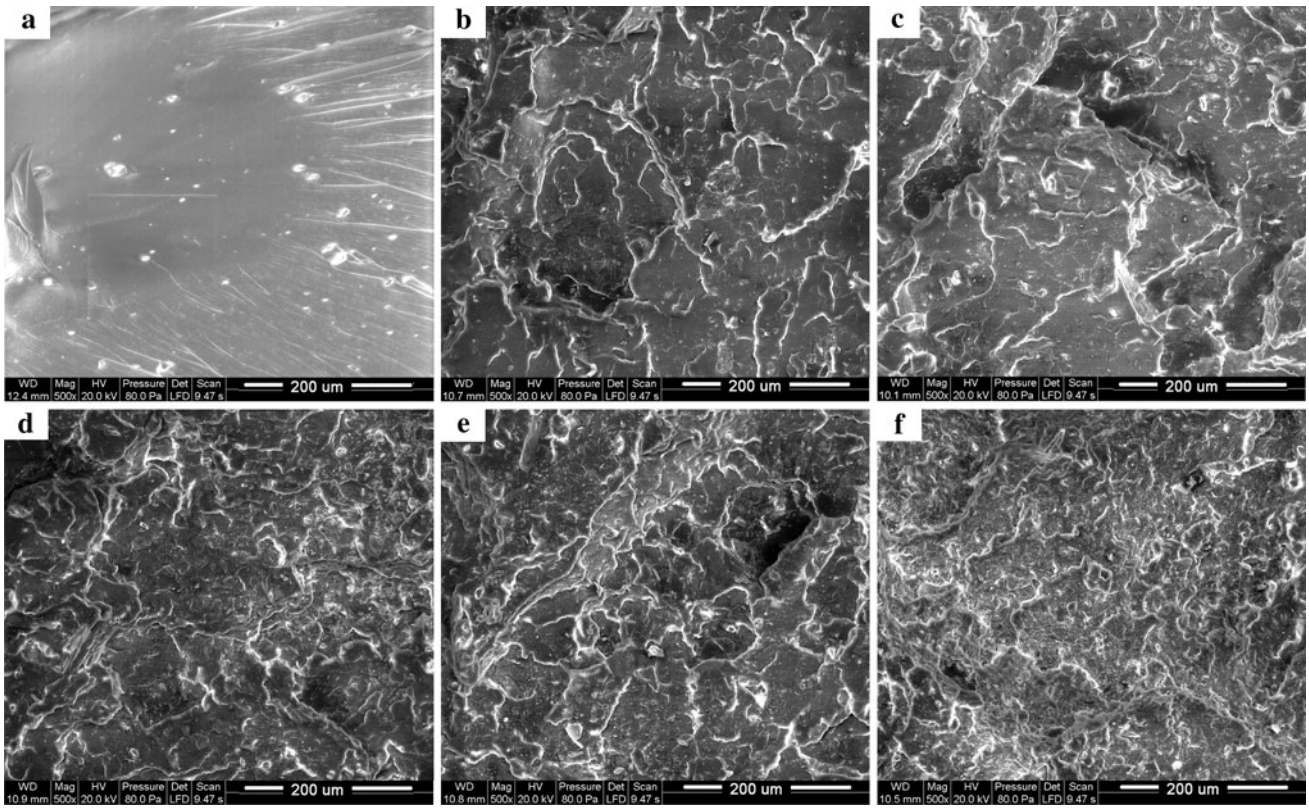

Fig. 10 SEM micrographs of tensile-fractured surfaces of PLA/CEL blends with various weight contents of CEL: **a** 0%, **b** 5%, **c** 10%, **d** 20%, **e** 30%, and **f** 40%

[11, 38, 39] between PLA carbonyls and the hydroxyl groups on lignin and cellulose chains that enhances the interfacial interaction between the CEL and the PLA.

Figure 10 shows the morphology of the tensile-fractured surfaces of neat matrix PLA and its blends with different contents of CEL. It is found that the surfaces of PLA and the blends are smooth, indicating a typical fragile breakage of neat PLA and the blends. The difference on the surface morphology between the neat PLA and the blends is that, the tensile-fractured surface of neat PLA is uniform, whereas the continuous PLA phase in the blends is uniformly interrupted by the increasing CEL filler. However, the uniform breakage on the tensile-fractured surface of the blends further confirms good dispersal of the CEL in the matrix; and the pulled CEL particles covered with matrix and the caves left on the tensile-fractured surfaces of the blends can confirm the good adhesion of the CEL and the PLA.

In order to get more information about the intermolecular interactions between CEL and PLA, the blends with 30 and 40 wt% CEL were measured with FTIR. IR spectra of the blends and neat PLA and CEL were compared in Fig. 11. The monomeric repeating unit of PLA contains a carbonyl group, yielding a strong IR C=O stretching mode band near 1,760 cm^{-1}; and the chain-end hydroxyl groups of PLA shows a moderate absorption near 3,400 cm^{-1}. While in the spectrum of the CEL, the absorption near 1,760 cm^{-1} is too weak to be noticed when compared to that of the PLA, but there is a strong absorption band near 3,400 cm^{-1} attributed to the O–H stretching of the hydroxyl groups. This peak is attributed to the phenolic hydroxyl groups in lignin. And these phenolic hydroxyl groups have a strong ability to form hydrogen bonds with the carbonyl groups. Thus, the change in FT-IR spectra at about 1,760 cm^{-1} can be attributed directly to the change of the chemical environment for the carbonyl groups such as the formation of hydrogen bonds between the hydroxyl groups of the CEL and the carbonyl groups of the PLA. However, in this case, the change in the regions near 3,400 cm^{-1} can be not only from the formation of intermolecular hydrogen bonds between the PLA and the CEL, but also related to the ratios of the components in the blends.

From Fig. 11, it can be seen that the strength and the position of O–H stretching vibration for the blend are difference from that of the PLA or the CEL, but it is very difficult for us to form a very affirmative conclusion about the existence of intermolecular hydrogen bonds between PLA and CEL for the above reasons. However, carbonyl groups of PLA produced strong absorption at around

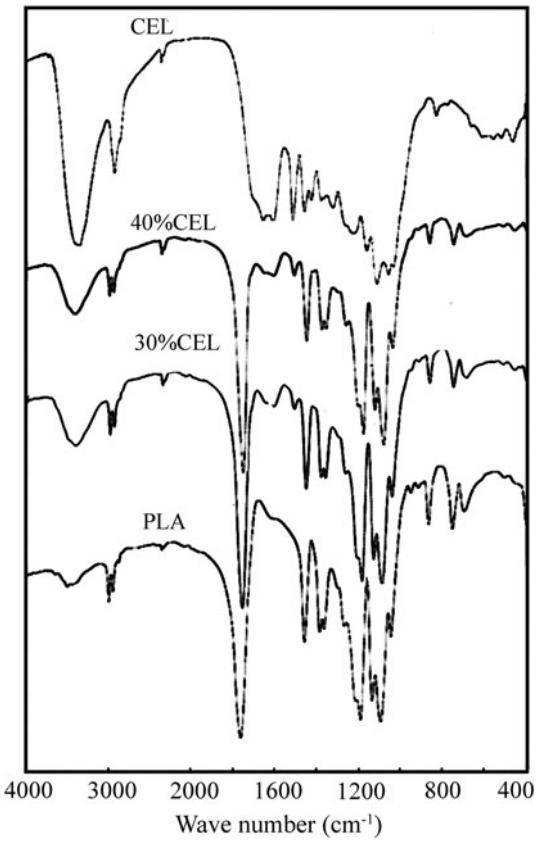

Fig. 11 IR spectra of PLA, CEL, and their blends

1,760 cm^{-1} and there is a very small lower shift with increasing CEL content in the blends, indicating the formation of intermolecular hydrogen bonds between the CEL and the PLA molecules in this case. But the shift was very small probably due to the fact that PLA and CEL are not miscible at the molecular level and the number of phenol groups in the lignin would be too small to exert a serious influence on the carbonyl absorption.

Conclusions

CEL could be well dispersed in PLA by melt extrusion blending. There were efficient H-bond interactions between the PLA and the CEL components in the blends, resulting in retainment of PLA's thermal and mechanical properties in PLA/CEL blends. It was suggested that CEL is a potential material to be used as excellent filler in PLA-based products. This result will expand the consumer applications of PLA and promote the fabrication of low-cost and eco-friendly polymer materials.

Acknowledgments The financial support of National Natural Science Foundation of China (Grant No. 50821062) was greatly appreciated. The authors would like to thank Prof. Yong Qiang in Nanjing University of Forest for his gift of the CEL sample, Prof. Mingcai Chen in Guangzhou Institute of Chemistry, CAS for the assistance in blending processing, and Dr. Linli Xu for her helpful discussion.

References

1. Amass W, Amass A, Tighe B (1998) Polym Int 47:89
2. Inoue Y, Yoshie N (1992) Prog Polym Sci 17:571
3. Li JC, He Y, Inoue Y (2001) Polym J 33:336
4. Nampoothiri KM, Nair NR, John R (2010) Bioresour Technol 101:8493
5. Mooney BP (2009) Biochem J 418:219
6. Nyambo C, Mohanty AK, Misra M (2010) Biomaromolecules 11:1654
7. Auras R, Harte B, Selke S (2004) Macromol Biosci 4:835
8. Koning C, van Duin M, Pagnoulle C, Jerome R (1998) Prog Polym Sci 23:707
9. Ciemniecki SL, Glasser WG (1988) Polymer 29:1021
10. Ciemniecki SL, Glasser WG (1988) Polymer 29:1030
11. Li J, He Y, Inoue YS (2003) Polym Int 52:949
12. Yokohara T, Yamaguchi M (2008) Eur Polym J 44:677
13. Takagi Y, Yasuda R, Yamaoka M, Yamane T (2004) J Appl Polym Sci 93:2363
14. Yeh JT, Tsou CH, Huang CY, Chen KN, Wu CS, Chai WL (2010) J Appl Polym Sci 116:680
15. Yuan H, Liu ZY, Ren J (2009) Poly Eng Sci 49:1004
16. Liu XX, Khor S, Petinakis E, Yu L, Simon G, Dean K, Bateman S (2010) Thermochim Acta 509:147
17. Mohamed AA, Gordon SH, Carriere CJ, Kim S (2006) J Food Qual 29:266
18. Wang N, Yu JG, Ma XF (2007) Polym Int 56:1440
19. Huneault MA, Li HB (2007) Polymer 48:270
20. Wang N, Yu JG, Chang PR, Ma XF (2008) Carbohydr Polym 71:109
21. Pradhan R, Misra M, Erickson L, Mohanty A (2010) Bioresour Technol 101:8489
22. Finkenstadt VL, Tisserat B (2010) Ind Crops Prod 31:316
23. Chen DK, Li J, Ren J (2010) Compos Part A–Appl S 41:101
24. Chakraborty A, Sain M, Kortschot M, Cutler S (2007) J Biobased Mater Bioenergy 1:71
25. Zhang YC, Wu HY, Qiu YP (2010) Bioresource Technol 101:7944
26. Xu J, Zhang JH, Gao WQ, Liang HW, Wang HY, Li JF (2009) Mater Lett 63:658
27. Peesan M, Supaphol P, Rujiravanit R (2005) Carbohyd Polym 60:343
28. Liao HT, Wu CS (2009) Mat Sci Eng A-Struct 515:207
29. Ren J, Fu HY, Ren TB, Yuan WZ (2009) Carbohyd Polym 77:576
30. Sarazin P, Li G, Orts WJ, Favis BD (2008) Polymer 49:599
31. Liu X, Dever M, Fair N, Benson RS (1997) J Environ Polym Degr 5:225
32. Ke TY, Sun XZS (2003) J Polym Environ 11:7
33. Kumar MNS, Mohanty AK, Erickson L, Misra M (2009) J Biobased Mater Bioenergy 3:1
34. Corradini E, Pineda EAG, Hechenleitner AAW (1999) Polym Degrad Stabil 66:199
35. Teramoto Y, Lee SH, Endo T (2009) Polym J 41:219
36. Petinakis E, Liu XX, Yu L, Way C, Sangwan P, Dean K, Bateman S, Edward G (2010) Polym Degrad Stabil 95:1704
37. Liu LF, Yu JY, Cheng LD, Qu WW (2009) Compos Part A-Appl S 40:669
38. Cao X, Mohamed A, Gordon SH, Willett JL, Sessa DJ (2003) Thermochim Acta 406:115
39. Finkenstadt VL, Liu LS, Willett JL (2007) J Polym Environ 15:1